pp 457–472. © Royal Aeronautical Society 2016
doi: 10.1017/aer.2016.5

Robust and simple intelligent observer-based fault estimation and reconstruction for a class of non-linear systems: HIRM aircraft

M.H. Khooban
mhkhoban@gmail.com, khooban@sutech.ac.ir
Young Researchers and Elite Club, Garmsar Branch
Islamic Azad University, Garmsar
Iran

M. Siahi
Department of Electrical Engineering, Garmsar Branch
Islamic Azad University, Semnan
Iran

M.-R. Soltanpour
Department of Electrical Engineering
Aeronautical University of Science and Technology, Tehran
Iran

ABSTRACT

This paper introduces an observer strategy, namely a Sliding Mode Observer (SMO), to realise the fault detection and estimation of general uncertain non-linear systems. The use of a non-linear observer is considered for monitoring the states of a high incidence research model (HIRM) aircraft system. For a special class of Lipschitz non-linear system, a fault reconstruction scheme is presented where the reconstructed signal can approximate the fault signal to any accuracy. The proposed method is based only on the available plant input-output information and can be calculated online. Moreover, the globally asymptotic stability of the closed-loop system is mathematically proved. Finally, an HIRM aircraft system example is given to illustrate the efficiency of the proposed approach.

Keywords: Sliding mode observer; Non-linear systems; State estimation; Fault reconstruction; HIRM Aircraft

Received 17 July 2015; revised 3 September 2015; accepted 10 September 2015.

https://doi.org/10.1017/aer.2016.5 Published online by Cambridge University Press

1.0 INTRODUCTION

As automatic control systems can be very effective in reducing energy losses, they are widely used in industrial fields. However, such systems are susceptible to poor performance because the interaction between the human operator and the systems is often ignored. Also, unanticipated changes in the external environment can make the system defective. The effect of faults can be destructive if they are not detected early. So, practical fault detection and isolation (FDI) methods are essential. The primary task of FDI methods is to show that something is incorrect and specify which component has a fault. Progress in modelling methods has raised the possibility of applying model-based FDI methods. These have been considered a very efficient approach for FDI both in theory and in practice(1).

The control of uncertain systems exposed to an external perturbation has become an active field of study during the past decade. Most of the systems encountering problems of this kind in real terms are usually affected by various uncertainties such as parameter variations, actuator faults and non-linearities. In the majority of control strategies proposed in literature, it is assumed that all state variables are available. However, this is not always true in practice. Hence, a state vector needs to be estimated to be used in the control rules. The fault identification plan is mainly aimed at producing a warning when faults occur(2). Among the common methods used to perform comparisons in this field are the Kalman filter(3), adaptive observers(4), high-gain observers(5) and sliding mode observers (SMO)(6-9).

The SMO takes advantage of discontinuous control actions to move the observer error direction towards a certain hyper-plane in the fault space; from this point, the direction of the slide is maintained until the fault states converge to the origin. Basically, the observer generates the signals used to discover data associated with the fault. Remaining generation statements, used as linear observers, have been extensively applied. In this method, discrepancy between the system output and observer output is processed by a weighting matrix to form so called residuals. The remaining will equal zero if a fault does not occur in the process. However, it will reply specifically once a special fault occurs(10,11).

In 1992, Utkin et al designed an ordinary observer with a discontinuous part that was fed back along with an appropriate gain(12). An observer where the output fault is fed back linearly was designed by Walcott and Zakin(13), and a Lyapunov technique was applied to show its sustainability. A canonical form was proposed by Spurgeon and Edwards(14,15) for the design of an SMO that depends on the invariable zeros of the system and the particular conditions related to the input and output distribution matrices. They used both the linear and non-linear output error injection in that procedure. They also presented a procedure for calculating the linear output error injection gain. The solution is obvious. However, it does not make use of all the degrees of freedom. In Ref. 16, another canonical form was suggested by Edwards et al based on an adequate status in accordance with the linear matrix inequality (LMI). In that paper, the authors tried to utilise the freedom in the model proposed by Edwards(17) for sectional pole attribution. However, they did not determine the best position for eigenvalues in the region of interest.

In recent years, the sliding-mode method has been used widely to design controllers or state observers(18-22). Sliding-mode method has been used in many studies(18,19) to control linear time invariant (LTI) and time variant systems (LTV) with uncertainties. In these studies, the superiority of the proposed methods is well-presented. But unfortunately, these methods cannot be used for non-linear systems due to the unstructured nature of uncertainties in them. Therefore, to have an effective control technique for linear systems, to overcome the uncertainties and to ensure the stability of the closed-loop system, control input coefficients

https://doi.org/10.1017/aer.2016.5 Published online by Cambridge University Press

must be increased. This, in turn, will lead to an increase in control input amplitude and consequently the saturation of actuators. In Refs 20-22, sliding-mode method was used as the controller or state observer in non-linear systems with uncertainty. Mathematical proof and simulation results have shown the acceptable performance of these methods. But in these studies, unlike the conventional methods, the integral of system states is used to determine the sliding surface. The use of an integral factor in a sliding surface will lead to an undesirable wind-up effect. So, the practical implementation of these methods will encounter problems[(23-27)].

It must be emphasised that 'accurate' fault reconstruction is very encouraging in non-linear systems, particularly in the presence of uncertainty. The notion of 'accurate' fault reconstruction has been considered by Edwards[(14)] for linear systems without uncertainty. When uncertainties are considered, all the sliding mode observer-based fault reconstruction results offer only an estimate of the fault signal. It is highly desirable to create a procedure for fault reconstruction in non-linear systems or to achieve conditions under which 'accurate' fault reconstruction is possible. Also, since FDI is needed for use in real engineering systems, the reconstruction fault signal needs to be based only on accessible measured data.

In this study, a simple SMO is proposed for a special of class of non-linear systems in the presence of faults/unknown inputs. All the parametric uncertainties/disturbances present in the system are modelled in the form of unknown inputs/faults. The unknown input can be a combination of immeasurable or unmeasured disturbances, unknown control actions, or un-modelled system dynamics. The novelty of this study lies in the choice of robust terms to deal with faults/unknown inputs. The methods of the researches use all the output information to deal with unknown inputs, and so require the reduced-order system itself to be stable in the sliding mode[(15,28-30)]. Moreover, the robust terms are applied to 'reconstruct' all the faults/unknown inputs from the sliding mode. Finally, an HIRM aircraft system example is given to illustrate the efficiency of the proposed approach.

The organisation of this paper is as follows:

In Section 2, the dynamic equations of a non-linear system and necessary assumptions for the design of an SMO are introduced. In Section 3, the design details of the SMO are described. Section 4 discusses the selection of the sliding surface and the necessary conditions for existence of the sliding surface. In Section 5, using mathematical analysis, we try to obtain the conditions for making the error zero. In Section 6, fault reconstruction using the sliding mode is explained. In Section 7, the advantages of the proposed method are explained. In Section 8, the dynamic equations of the HIRM aircraft system are introduced. The simulation results of the proposed observer are presented and discussed in Section 9. Finally, conclusions are drawn in Section 10.

2.0 FORMULATING THE PROBLEM

Consider the following system[(31)]:

$$\begin{aligned} \dot{\boldsymbol{x}}(\boldsymbol{t}) &= \boldsymbol{A}x + \boldsymbol{g}(\boldsymbol{x}, \boldsymbol{u}) + \boldsymbol{E}(\boldsymbol{x}, \boldsymbol{u})\, \boldsymbol{f}(\boldsymbol{t}) \\ \boldsymbol{y}(\boldsymbol{t}) &= \boldsymbol{C}x, \end{aligned} \qquad \ldots (1)$$

where $x \in R^n$ is the state vector; $u \in R^q$ is the input vector and $y \in R^p$ is the output vector; $f(t) \in R^m$ shows the actuator fault; A, C and E are known constant real matrices of suitable dimensions; the pair (A, C) are observable; $g(x, u)$ is a continuous non-linear vector function, assumed to be Lipschitz, with a Lipschitz constant l_g, i.e. $\|g(\hat{x},u) - g(x,u)\| \leq l_g \|\hat{x} - x\|$. It

https://doi.org/10.1017/aer.2016.5 Published online by Cambridge University Press

is assumed that the derivative of $f(t)$ with respect to time is norm-bounded, i.e. $\|\dot{f}(t)\| \leq f_1$, where $f_1 \geq 0$.

Assumption 1: Matrix $\boldsymbol{C}$ is a full rank matrix and the pair $(\boldsymbol{A}, \boldsymbol{C})$ is observable.

Thanks to $\boldsymbol{C}$ being a full rank matrix, we consider that the first $\boldsymbol{m}$ rows (outputs) of matrix $\boldsymbol{C}$ form a full rank $\boldsymbol{m} \times \boldsymbol{n}$ matrix $\boldsymbol{C}_1$ such that

$$\boldsymbol{C}_1 = [\boldsymbol{C}_{11}\ \boldsymbol{C}_{12}]_{\boldsymbol{m}\times\boldsymbol{n}};\ \boldsymbol{Rank}[\boldsymbol{C}_{11}]_{\boldsymbol{m}\times\boldsymbol{m}} = \boldsymbol{m}.$$

Thus, Rank $(\boldsymbol{C}_1) = \boldsymbol{m}$. By partitioning the output distribution matrix, the following equations could be obtained:

$$\boldsymbol{y} = \begin{bmatrix} \boldsymbol{C}_1 \\ \boldsymbol{C}_2 \end{bmatrix} \boldsymbol{x},\quad \boldsymbol{y}_1 = \boldsymbol{C}_1 \boldsymbol{x}.$$

The following result depends on the observability of faults/unknown inputs from measurements of the output. The following assumptions on the fault distribution matrix are the basic needs for the expansion of the SMO that can use the faults in the sliding mode.

Assumption 2: The function $\boldsymbol{E}(\boldsymbol{x}, \boldsymbol{u})$ and the inverse of the non-linear matrix $\boldsymbol{C}_1\boldsymbol{E}(\boldsymbol{x}, \boldsymbol{u})$, exist and are bounded $\forall \boldsymbol{x} \in \boldsymbol{M}$ and $\boldsymbol{u} \in \boldsymbol{U}$.

Assumption 3: The non-linear functions $g(\boldsymbol{x}, \boldsymbol{u})$ and $\boldsymbol{E}(\boldsymbol{x}, \boldsymbol{u})$ fulfil the Lipschitz conditions so that

$$\begin{aligned}&\|\boldsymbol{g}(\hat{x}, \boldsymbol{u}) - \boldsymbol{g}(\boldsymbol{x}, \boldsymbol{u})\| \leq \boldsymbol{l}_\phi \|\hat{x} - \mathbf{x}\| \, \|\boldsymbol{E}(\hat{x}, \boldsymbol{u})(\boldsymbol{C}_1\boldsymbol{E}(\hat{x}, \boldsymbol{u}))^{-1} \\ &-\boldsymbol{E}(\boldsymbol{x}, \boldsymbol{u})(\boldsymbol{C}_1\boldsymbol{E}(\boldsymbol{x}, \boldsymbol{u}))^{-1}\| \leq \boldsymbol{l}_g \|\hat{x} - \mathbf{x}\|\end{aligned}$$

for some Lipschitz constants $\boldsymbol{l}_\phi$ and $\boldsymbol{l}_g$.

Remark 1: In this paper, all parametric uncertainties/disturbances affecting the system are modelled as unknown inputs/faults. In order to generalise the expansion, the fault distribution matrix $\boldsymbol{E}(\boldsymbol{x}, \boldsymbol{u})$ is intended to be non-linear without any constraint.

3.0 THE DESIGN OF THE SLIDING MODE OBSERVER

For Equation (1), an observer, as follows, can be developed to estimate the states:

$$\hat{x} = \boldsymbol{A}\hat{x} + \boldsymbol{g}(\hat{x}, \boldsymbol{u}) + \boldsymbol{L}(\boldsymbol{y} - \boldsymbol{C}\hat{x}) + \boldsymbol{E}(\hat{x}, \boldsymbol{u})\, \boldsymbol{v}(\boldsymbol{t}), \qquad \ldots (2)$$

where L is the feedback gain and $\boldsymbol{v}(t)$ is the robust term provided by the sliding-mode estimation[31]:

$$\boldsymbol{v}(\boldsymbol{t}) = -(\boldsymbol{C}_1\boldsymbol{E}(\hat{x}, \boldsymbol{u}))^{-1} \rho(0)\ \boldsymbol{sign}\ (\boldsymbol{C}_1\hat{x} - \boldsymbol{C}_1\boldsymbol{x}). \qquad \ldots (3)$$

Also, $\rho(.)$ is a positive scalar function that needs to be specified.

Remark 2: In the above observer development, the disturbance inputs are substituted by robust terms. The number of robust terms $\boldsymbol{v}(t)$ is equivalent to the number of fault inputs $f_i(t)$.

By defining the estimation error as $e = \hat{x} - x$, the estimation error dynamics can be calculated from Equations (1) and (2) as

$$\dot{e} = (A - LC)\, e + g(\hat{x}, u) - g(x, u) + E(\hat{x}, u)\, v(t) - E(x, u)\, f(t). \qquad \dots (4)$$

Because the non-linear matrix $E(.)$ and faults $f(t)$ are limited, the boundedness of the error dynamics can be ensured with an appropriate selection of feedback gain L using the standard Lyapunov analysis.

4.0 DESIGN OF SLIDING MODE SURFACE FOR FAULT DETECTION

The selection of sliding-mode gain ρ(.) to guarantee the existence of the sliding mode will be reviewed in this section. The main purpose of the robust terms $v(t)$ in Equation (2) is to compensate for fault inputs and improve the integrity of estimation. This approach can be expressed as follows:

1. Describe the following sliding surfaces[31]:

$$e_{y1} = C_1 e = 0; \text{ that is, } e_{yi} = 0, \text{ for all } i = 1, 2, \dots, m. \qquad \dots (5)$$

2. Design the sliding-mode estimation as Equation (2) with $v(t)$ presented by Equation (3) so that the system can achieve the sliding mode.
3. Make sure that the reduced-order estimation error dynamics goes toward zero on the sliding surfaces of $e_{y1} = 0, e_{y2} = 0, \dots, e_{ym} = 0$.

By defining $e_y = C_1 e$, we have

$$\dot{e}_y = C_1\dot{e} = C_1(A - LC)\, e + C_1 g(\hat{x}, u) - C_1 g(x, u) + C_1 E(\hat{x}, u)\, v(t) - C_1 E(x, u)\, f(t). \qquad \dots (6)$$

By inserting Equation (4) into Equation (6), we have

$$\dot{e}_y = C_1(A - LC)\, e + C_1 g(\hat{x}, u) - C_1 g(x, u) - \rho(0)\ sign\left(e_y\right) - C_1 E(x, u)\, f(t). \qquad \dots (7)$$

The stability of the reduced-order dynamics can be easily analysed in the transformed domain. From Assumptions 1 and 2, we have $\boldsymbol{det}(C_{11}) \neq 0$; then, there exists a non-singular transformation

$$T = \begin{bmatrix} C_{11} & C_{12} \\ 0 & I_{n-m} \end{bmatrix}, \qquad \dots (8)$$

https://doi.org/10.1017/aer.2016.5 Published online by Cambridge University Press

with the following transformed matrices:

$$\begin{aligned}
&\boldsymbol{TAT}^{-1} = \tilde{\boldsymbol{A}} = \begin{bmatrix} \tilde{\boldsymbol{A}}_{11} & \tilde{\boldsymbol{A}}_{12} \\ \tilde{\boldsymbol{A}}_{21} & \tilde{\boldsymbol{A}}_{22} \end{bmatrix}, \ \boldsymbol{C}_1\boldsymbol{T}^{-1} = [\boldsymbol{I}_m \ 0] \\
&\boldsymbol{y} = \begin{bmatrix} \boldsymbol{C}_1 \\ \boldsymbol{C}_2 \end{bmatrix} \boldsymbol{T}^{-1}\boldsymbol{x} = \begin{bmatrix} \boldsymbol{y}_1 \\ \boldsymbol{y}_2 \end{bmatrix}, \ \boldsymbol{y}_1 = \boldsymbol{x}_1, \ \boldsymbol{y}_2 = \tilde{\boldsymbol{C}}_2\boldsymbol{x} \\
&\boldsymbol{T}L\begin{bmatrix} \boldsymbol{C}_1 \\ \boldsymbol{C}_2 \end{bmatrix} \boldsymbol{T}^{-1} = \boldsymbol{H} = \begin{bmatrix} \boldsymbol{H}_{11} & \boldsymbol{H}_{12} \\ \boldsymbol{H}_{21} & \boldsymbol{H}_{22} \end{bmatrix} \\
&\boldsymbol{T}g(\boldsymbol{x},\boldsymbol{u}) = \boldsymbol{\Gamma}(\boldsymbol{x},\boldsymbol{u}) = \begin{bmatrix} \boldsymbol{\Gamma}_1(\boldsymbol{x},\boldsymbol{u}) \\ \boldsymbol{\Gamma}_2(\boldsymbol{x},\boldsymbol{u}) \end{bmatrix} \\
&\boldsymbol{T}E(\boldsymbol{x},\boldsymbol{u}) = \tilde{\boldsymbol{E}}(\boldsymbol{x},\boldsymbol{u}) = \begin{bmatrix} \tilde{\boldsymbol{E}}_1(\boldsymbol{x},\boldsymbol{u}) \\ \tilde{\boldsymbol{E}}_2(\boldsymbol{x},\boldsymbol{u}) \end{bmatrix},
\end{aligned} \qquad \ldots (9)$$

where x_1 is measurable output.

Now, we have $\boldsymbol{C}_1\boldsymbol{E}(\boldsymbol{x},\boldsymbol{u}) = \tilde{\boldsymbol{E}}_1(\boldsymbol{x},\boldsymbol{u})$. By defining $\tilde{\boldsymbol{e}} = \boldsymbol{T}e = [e_y^T \ \tilde{e}_2^T]^T$, we transform the error dynamics of Equation (7) with the transformation in Equation (8) to the form

$$\begin{aligned}
\dot{\boldsymbol{e}}_y = {} & \left(\tilde{\boldsymbol{A}}_{11} - \boldsymbol{H}_{11}\right)\boldsymbol{e}_y + \left(\tilde{\boldsymbol{A}}_{12} - \boldsymbol{H}_{12}\right)\boldsymbol{e}_2 + \boldsymbol{\Gamma}_1(\tilde{\boldsymbol{x}},\boldsymbol{u}) - \boldsymbol{\Gamma}_1(\boldsymbol{x},\boldsymbol{u}) - \boldsymbol{\rho}(0)\,sign\left(\boldsymbol{e}_y\right) \\
& - \tilde{\boldsymbol{E}}_1(\boldsymbol{x},\boldsymbol{u})\,\boldsymbol{f}(\boldsymbol{t})
\end{aligned} \qquad \ldots (10)$$

$$\begin{aligned}
\tilde{\boldsymbol{e}}_2 = {} & \left(\tilde{\boldsymbol{A}}_{21} - \boldsymbol{H}_{21}\right)\boldsymbol{e}_y + \left(\tilde{\boldsymbol{A}}_{22} - \boldsymbol{H}_{22}\right)\boldsymbol{e}_2 + \boldsymbol{\Gamma}_2(\tilde{\boldsymbol{x}},\boldsymbol{u}) - \boldsymbol{\Gamma}_2(\boldsymbol{x},\boldsymbol{u}) + \tilde{\boldsymbol{E}}_2(\tilde{\boldsymbol{x}},\boldsymbol{u})\,\boldsymbol{v}(\boldsymbol{t}) \\
& - \tilde{\boldsymbol{E}}_2(\boldsymbol{x},\boldsymbol{u})\,\boldsymbol{f}(\boldsymbol{t}),
\end{aligned} \qquad \ldots (11)$$

where $\boldsymbol{H}$ is the feedback gain matrix in the transformed domain. According to the transformation, all the states in the subsystem e_y are measurable. Considering the generality of the problem, $\boldsymbol{H}_{11}$ can be chosen to be of full rank.

Lemma 1: *For the systems of Equations* (10) *and* (11) *fulfilling Assumptions* 1-3 *are driven to the sliding surface of Equation* (5) *in limited time and stay on it if the sliding-mode gain* $\rho(.)$ *in Equation (7) fulfils*

$$\boldsymbol{\rho}(\hat{\boldsymbol{x}},\boldsymbol{x},\boldsymbol{u}) \geq \left(\left\|\tilde{\boldsymbol{A}}_{12} - \boldsymbol{H}_{12}\right\| + \boldsymbol{l}_{\boldsymbol{\Gamma}_1}\right)\boldsymbol{b}_e + \boldsymbol{b}_{\tilde{E}_1}\bar{\boldsymbol{f}} + \boldsymbol{\beta}, \qquad \ldots (12)$$

where $\|e\| \leq b_e$ and β is a positive constant.

Proof: Consider the Lyapunov function $V_1 = 1/2e_y^T e_y$, differentiating with respect to time and using Equation (11), we have[31]

$$\begin{aligned}
\dot{V}_1 \leq \boldsymbol{e}_y^T\dot{\boldsymbol{e}}_y = \boldsymbol{e}_y^T & \left[\left(\tilde{\boldsymbol{A}}_{12} - \boldsymbol{H}_{12}\right)\tilde{\boldsymbol{e}}_2 - \tilde{\boldsymbol{E}}_1(\boldsymbol{x},\boldsymbol{u})\,\boldsymbol{f}(\boldsymbol{t}) + \boldsymbol{\Gamma}_1(\tilde{\boldsymbol{x}},\boldsymbol{u}) - \boldsymbol{\Gamma}_1(\boldsymbol{x},\boldsymbol{u})\right] \\
& + \boldsymbol{e}_y^T\left(\tilde{\boldsymbol{A}}_{11} - \boldsymbol{H}_{11}\right)\boldsymbol{e}_y - \boldsymbol{\rho}(0)\left\|\left(\boldsymbol{e}_y\right)\right\|.
\end{aligned} \qquad \ldots (13)$$

https://doi.org/10.1017/aer.2016.5 Published online by Cambridge University Press

From Assumption 2, we have $\|\tilde{\boldsymbol{E}}_1(\boldsymbol{x},\boldsymbol{u})\| \le b_{\tilde{E}_1}$ for some upper bound $b_{\tilde{E}_1}$. From the Lipschitz condition in Assumption 3, we have $\|\Gamma_1(\tilde{\boldsymbol{x}},\boldsymbol{u}) - \Gamma_1(\boldsymbol{x},\boldsymbol{u})\| \le l_{\Gamma_1}$ for some Lipschitz constant l_{Γ_1}.

$$\dot{V}_1 \le \|\boldsymbol{e}_y\| \left[\left\| \tilde{\boldsymbol{A}}_{12} - \boldsymbol{H}_{12} \right\| + \boldsymbol{l}_{\Gamma_1} \right) \boldsymbol{b}_e + \boldsymbol{b}_{\tilde{E}_1} \bar{\boldsymbol{f}}] + \; e_y^{\boldsymbol{T}} \left(\tilde{\boldsymbol{A}}_{11} - \boldsymbol{H}_{11} \right) \boldsymbol{e}_y - \rho\,(0) \left\| \left(\boldsymbol{e}_y \right) \right\| \quad \ldots (14)$$

From Equation (14) we conclude that

$$\dot{V}_1 \le \boldsymbol{e}_y^{\boldsymbol{T}} \left(\tilde{A}_{11} - \boldsymbol{H}_{11} \right) \boldsymbol{e}_y - \beta \left(\boldsymbol{e}_y \right).$$

Because $\boldsymbol{H}_{11}$ is of full rank, we can choose $\boldsymbol{H}_{11}$ such that $\tilde{\boldsymbol{A}}_{11} - \boldsymbol{H}_{11} = \boldsymbol{P}_1$, where $\boldsymbol{P}_1 > 0$ is positive definite. So,

$$\dot{V}_1 \le -\boldsymbol{e}_y^{\boldsymbol{T}} \boldsymbol{P}_1 \boldsymbol{e}_y - \beta \left\| \left(\boldsymbol{e}_y \right) \right\| < 0.$$

Thus, the gain in Equation (14) guarantees that the sliding surface can be achieved in a limited time.

5.0 CHECK THE ERROR CONVERGENCE IN THE PROPOSED METHOD

By substituting the tantamount output error infusion signal into the error dynamics Equation (8), the error dynamics in the sliding mode could be obtained[31]. In the sliding mode $e_y = 0$, we have $\dot{e}_y = 0$. So, the tantamount output error infusion signal of $v(t)$, veq can be obtained from Equation (10) according to[6] as follows:

$$\boldsymbol{0} = \; \boldsymbol{C}_1 \left(\boldsymbol{A} - \boldsymbol{L}\boldsymbol{C} \right) \boldsymbol{e} + \boldsymbol{C}_1 \boldsymbol{g} \left(\tilde{\boldsymbol{x}}, \boldsymbol{u} \right) - \boldsymbol{C}_1 \boldsymbol{g} \left(\boldsymbol{x}, \boldsymbol{u} \right) + \boldsymbol{C}_1 \boldsymbol{E} \left(\tilde{\boldsymbol{x}}, \boldsymbol{u} \right) \boldsymbol{v}_{eq} - \boldsymbol{C}_1 \boldsymbol{E} \left(\boldsymbol{x}, \boldsymbol{u} \right) \boldsymbol{f} \left(\boldsymbol{t} \right) \quad \ldots (15)$$

So,

$$\begin{aligned} \boldsymbol{v}_{eq} = &\left(\boldsymbol{C}_1 \boldsymbol{E} \left(\tilde{\boldsymbol{x}}, \boldsymbol{u} \right) \right)^{-1} \boldsymbol{C}_1 \boldsymbol{E} \left(\boldsymbol{x}, \boldsymbol{u} \right) \boldsymbol{f} \left(\boldsymbol{t} \right) - \left(\boldsymbol{C}_1 \boldsymbol{E} \left(\tilde{\boldsymbol{x}}, \boldsymbol{u} \right) \right)^{-1} \times \left(\boldsymbol{C}_1 \left(\boldsymbol{A} - \boldsymbol{L}\boldsymbol{C} \right) \boldsymbol{e} + \boldsymbol{C}_1 \boldsymbol{g} \left(\tilde{\boldsymbol{x}}, \boldsymbol{u} \right) \right. \\ &\left. - \boldsymbol{C}_1 \boldsymbol{g} \left(\boldsymbol{x}, \boldsymbol{u} \right) \right). \end{aligned} \quad \ldots (16)$$

By replacing the tantamount output error infusion signal into the error dynamics Equation (8), we have the following estimation of error dynamics in the sliding mode of $e_y = 0$.

$$\begin{aligned} \dot{e} = &\left(\boldsymbol{A} - \boldsymbol{L}\boldsymbol{C} \right) \boldsymbol{e} + \boldsymbol{g} \left(\tilde{\boldsymbol{x}}, \boldsymbol{u} \right) - \boldsymbol{g} \left(\boldsymbol{x}, \boldsymbol{u} \right) + \boldsymbol{E} \left(\tilde{\boldsymbol{x}}, \boldsymbol{u} \right) \left(\boldsymbol{C}_1 \boldsymbol{E} \left(\tilde{\boldsymbol{x}}, \boldsymbol{u} \right) \right)^{-1} \boldsymbol{C}_1 \boldsymbol{E} \left(\boldsymbol{x}, \boldsymbol{u} \right) \boldsymbol{f} \left(\boldsymbol{t} \right) \\ &- \boldsymbol{E} \left(\boldsymbol{x}, \boldsymbol{u} \right) \boldsymbol{f} \left(\boldsymbol{t} \right) - \boldsymbol{E} \left(\tilde{\boldsymbol{x}}, \boldsymbol{u} \right) \left(\boldsymbol{C}_1 \boldsymbol{E} \left(\tilde{\boldsymbol{x}}, \boldsymbol{u} \right) \right)^{-1} \left[\boldsymbol{C}_1 \left(\boldsymbol{A} - \boldsymbol{L}\boldsymbol{C} \right) \boldsymbol{e} + \boldsymbol{C}_1 \boldsymbol{g} \left(\tilde{\boldsymbol{x}}, \boldsymbol{u} \right) \right. \\ &\left. - \boldsymbol{C}_1 \boldsymbol{g} \left(\boldsymbol{x}, \boldsymbol{u} \right) \right] \end{aligned} \quad \ldots (17)$$

From the above error dynamics, it is obvious that the fault dynamics $\boldsymbol{E}(\tilde{\boldsymbol{x}},\boldsymbol{u})(\boldsymbol{C}_1\boldsymbol{E}(\tilde{\boldsymbol{x}},\boldsymbol{u}))^{-1}\boldsymbol{C}_1\boldsymbol{E}(\boldsymbol{x},\boldsymbol{u})\boldsymbol{f}(\boldsymbol{t}) - \boldsymbol{E}(\boldsymbol{x},\boldsymbol{u})f(t) \to 0$ as $\tilde{\boldsymbol{x}} \to \boldsymbol{x}$. Through an appropriate design of the feedback gain, the error dynamics can be stabilised. For convenience of analysis,

https://doi.org/10.1017/aer.2016.5 Published online by Cambridge University Press

feedback gain design that stabilises the error dynamics will be reviewed in the transformed domain. By assessment of the tantamount output error infusion signal from Equation (16) and replacing it in Equation (11), we have

$$\tilde{e}_2 = \left(\tilde{A}_{22} - \boldsymbol{H}_{22}\right)\tilde{e}_2 + \boldsymbol{\Gamma}_2(\tilde{\boldsymbol{x}}, \boldsymbol{u}) - \boldsymbol{\Gamma}_2(\boldsymbol{x}, \boldsymbol{u}) + \tilde{\boldsymbol{E}}_2(\tilde{\boldsymbol{x}}, \boldsymbol{u})\tilde{\boldsymbol{E}}_1^{-1}(\tilde{\boldsymbol{x}}, \boldsymbol{u})\tilde{\boldsymbol{E}}_1(\boldsymbol{x}, \boldsymbol{u})\boldsymbol{f}(\boldsymbol{t})$$
$$- \tilde{\boldsymbol{E}}_2(\tilde{\boldsymbol{x}}, \boldsymbol{u})\tilde{\boldsymbol{E}}_1^{-1}(\tilde{\boldsymbol{x}}, \boldsymbol{u})\left(\tilde{A}_{12} - \boldsymbol{H}_{12}\right)\tilde{e}_2 + \boldsymbol{\Gamma}_1(\tilde{\boldsymbol{x}}, \boldsymbol{u}) - \boldsymbol{\Gamma}_1(\boldsymbol{x}, \boldsymbol{u}) \qquad \dots(18)$$

$$= \left(\tilde{A}_{22} - \boldsymbol{H}_{22}\right)\tilde{e}_2 + \boldsymbol{\Gamma}_2(\tilde{\boldsymbol{x}}, \boldsymbol{u}) - \boldsymbol{\Gamma}_2(\boldsymbol{x}, \boldsymbol{u}) - \tilde{\boldsymbol{E}}_2(\tilde{\boldsymbol{x}}, \boldsymbol{u})\tilde{\boldsymbol{E}}_1^{-1}(\tilde{\boldsymbol{x}}, \boldsymbol{u})\left(\tilde{A}_{12} - \boldsymbol{H}_{12}\right)\tilde{e}_2$$
$$+ \boldsymbol{\Gamma}_1(\tilde{\boldsymbol{x}}, \boldsymbol{u}) - \boldsymbol{\Gamma}_1(\boldsymbol{x}, \boldsymbol{u}) + \Big[\tilde{\boldsymbol{E}}_2(\tilde{\boldsymbol{x}}, \boldsymbol{u})\tilde{\boldsymbol{E}}_1^{-1}(\tilde{\boldsymbol{x}}, \boldsymbol{u})$$
$$- \tilde{\boldsymbol{E}}_2(\tilde{\boldsymbol{x}}, \boldsymbol{u})\tilde{\boldsymbol{E}}_1^{-1}(\tilde{\boldsymbol{x}}, \boldsymbol{u})\tilde{\boldsymbol{E}}_1(\boldsymbol{x}, \boldsymbol{u})\boldsymbol{f}(\boldsymbol{t})\Big]. \qquad \dots(19)$$

The following Lemma 1 discusses the stability of reduced-order estimation error Equation (19) in the sliding mode.

Theorem 1: For the system (1) fulfilling Assumptions 1-3 and using the estimator (2), the sliding-mode gain (12) guarantees that the estimation error is asymptotically stable in the multiple sliding mode of $e_{\boldsymbol{y}1=0}, \dots, e_{ym}$ offered the gain $\boldsymbol{H}_{22}$ fulfils[31]

$$\left(\tilde{A}_{22} - \boldsymbol{H}_{22}\right)^{\boldsymbol{T}}\boldsymbol{P}_2 + \boldsymbol{P}_2\left(\tilde{A}_{22} - \boldsymbol{H}_{22}\right) = -\boldsymbol{I} \qquad \dots(20)$$

$$\boldsymbol{\lambda}_{\boldsymbol{max}}(\boldsymbol{P}_2) \le \frac{1}{2\boldsymbol{l}_{\boldsymbol{\alpha}}}, \qquad \dots(21)$$

where $l_\alpha \triangleq (l_{\Gamma 1} + b_{\gamma 1} l_{\Gamma 2} + b_{\gamma 2} + l_\gamma b_{E_1}\bar{f})$ for some Lipschitz constants $l_{\Gamma 1}, l_{\Gamma 2}, l_\gamma$ and some upper bounds $b_{\gamma 1}, b_{\gamma 2}, b_{\boldsymbol{E}_1}, \bar{f}$.

Proof: In the sliding mode, we have $e_y = 0$, so $\boldsymbol{e} \equiv [0e_2^T]^T$. Under the same Lipschitz conditions as in Assumption 3, we have

$$\begin{aligned}
&\left\|\tilde{\boldsymbol{E}}_2(\tilde{\boldsymbol{x}}, \boldsymbol{u})\tilde{\boldsymbol{E}}_2^{-1}(\tilde{\boldsymbol{x}}, \boldsymbol{u}) - \tilde{\boldsymbol{E}}_2(\boldsymbol{x}, \boldsymbol{u})\tilde{\boldsymbol{E}}_1^{-1}(\boldsymbol{x}, \boldsymbol{u})\right\| \le \boldsymbol{l}_{\boldsymbol{\gamma}}\|\boldsymbol{e}\| = \boldsymbol{l}_{\boldsymbol{\gamma}}\|\tilde{e}_2\| \\
&\|\boldsymbol{\Gamma}_1(\tilde{\boldsymbol{x}}, \boldsymbol{u}) - \boldsymbol{\Gamma}_1(\boldsymbol{x}, \boldsymbol{u})\| \le \boldsymbol{l}_{\boldsymbol{\Gamma}1}\|\boldsymbol{e}\| = \boldsymbol{l}_{\boldsymbol{\Gamma}1}\|\tilde{e}_2\| \\
&\|\boldsymbol{\Gamma}_2(\tilde{\boldsymbol{x}}, \boldsymbol{u}) - \boldsymbol{\Gamma}_1(\boldsymbol{x}, \boldsymbol{u})\| \le \boldsymbol{l}_{\boldsymbol{\Gamma}2}\|\boldsymbol{e}\| = \boldsymbol{l}_{\boldsymbol{\Gamma}2}\|\tilde{e}_2\|
\end{aligned} \qquad \dots(22)$$

for some Lipschitz constants $l_{\Gamma 1}$ and $l_{\Gamma 2}$. Because the known functions are bounded based on Assumption 2, we have

$$\begin{aligned}
&\left\|\tilde{\boldsymbol{E}}_2(\tilde{\boldsymbol{x}}, \boldsymbol{u})\tilde{\boldsymbol{E}}_2^{-1}(\tilde{\boldsymbol{x}}, \boldsymbol{u})\right\| \le \boldsymbol{b}_{\boldsymbol{\gamma}1} \\
&\left\|\tilde{\boldsymbol{E}}_2(\tilde{\boldsymbol{x}}, \boldsymbol{u})\tilde{\boldsymbol{E}}_1^{-1}(\tilde{\boldsymbol{x}}, \boldsymbol{u})\left(\tilde{A}_{12} - \boldsymbol{H}_{12}\right)\right\| \le \boldsymbol{b}_{\boldsymbol{\gamma}2} \\
&\left\|\tilde{\boldsymbol{E}}_1^{-1}(\tilde{\boldsymbol{x}}, \boldsymbol{u})\right\| \le \boldsymbol{b}_{\tilde{\boldsymbol{E}}_1}
\end{aligned} \qquad \dots(23)$$

https://doi.org/10.1017/aer.2016.5 Published online by Cambridge University Press

for some upper bounds $b_{\gamma 1}$, $b_{\gamma 2}$ and $b_{\tilde{E}_1}$. Now, we select the Lyapunov function candidate as $V_2 = \tilde{e}_2^T \boldsymbol{P}_2 e\, \tilde{e}_2$. Differentiating according to time, and by using Equation (19), we have

$$\begin{aligned}\dot{V}_2 &= \tilde{e}_2^T \boldsymbol{P}_2 \dot{e}_2 + \dot{e}_2^T \boldsymbol{P}_2 \tilde{e}_2 = \tilde{e}_2^T \left(\tilde{\boldsymbol{A}}_{22} - \boldsymbol{H}_{22}\right)^T \boldsymbol{P}_2 + \boldsymbol{P}_2 \left(\tilde{\boldsymbol{A}}_{22} - \boldsymbol{H}_{22}\right) \tilde{e}_2 \\ &+ 2\tilde{e}_2^T \boldsymbol{P}_2 \left[\boldsymbol{\Gamma}_2 (\tilde{\boldsymbol{x}}, \boldsymbol{u}) - \boldsymbol{\Gamma}_2 (\boldsymbol{x}, \boldsymbol{u}) - \tilde{\boldsymbol{E}}_2 (\tilde{\boldsymbol{x}}, \boldsymbol{u})\, \tilde{\boldsymbol{E}}_1^{-1} (\tilde{\boldsymbol{x}}, \boldsymbol{u}) \right. \\ &\quad \left. \times \left[\left(\tilde{\boldsymbol{A}}_{12} - \boldsymbol{H}_{12}\right) \tilde{e}_2 + \boldsymbol{\Gamma}_1 (\tilde{\boldsymbol{x}}, \boldsymbol{u}) - \boldsymbol{\Gamma}_1 (\boldsymbol{x}, \boldsymbol{u})\right]\right] \\ &+ 2\tilde{e}_2^T \boldsymbol{P}_2 \left[\tilde{\boldsymbol{E}}_2 (\tilde{\boldsymbol{x}}, \boldsymbol{u})\, \tilde{\boldsymbol{E}}_1^{-1} (\tilde{\boldsymbol{x}}, \boldsymbol{u}) - \tilde{\boldsymbol{E}}_2 (\boldsymbol{x}, \boldsymbol{u})\, \tilde{\boldsymbol{E}}_1^{-1} (\boldsymbol{x}, \boldsymbol{u})\right] \tilde{\boldsymbol{E}}_1 (\boldsymbol{x}, \boldsymbol{u})\, \boldsymbol{f} (\boldsymbol{t})\, .\end{aligned} \quad \ldots (24)$$

Considering the above results, we have

$$\dot{V}_2 \leq -\|\tilde{e}_2\|^2 + 2\boldsymbol{\lambda}_{max} (\boldsymbol{P}_2) \left[\boldsymbol{l}_{\Gamma 1} + \boldsymbol{b}_{\gamma 1} \boldsymbol{l}_{\Gamma 2} + \boldsymbol{b}_{\gamma 2} + \boldsymbol{l}_{\gamma} \boldsymbol{b}_{E_1} \bar{\boldsymbol{f}}\right] \|\tilde{e}_2\|^2.$$

If the estimation gain $\boldsymbol{H}$ is designed so that conditions in Equations (20) and (21) are fulfilled, the error dynamics in the sliding mode will be asymptotically stable.

Remark 3: If the fault distribution matrix $\tilde{\boldsymbol{E}}$ is a constant matrix or only involves functions of $\boldsymbol{y}_1$ outputs, that is, $\tilde{\boldsymbol{E}}(\boldsymbol{x}, \boldsymbol{u}) = \tilde{\boldsymbol{E}}(\boldsymbol{y}_1, \boldsymbol{u})$, then the reduced-order error dynamics will be completely free from faults. In the sliding mode, $e_y = 0$; therefore, $\tilde{\boldsymbol{E}}(\boldsymbol{x}^\wedge, \boldsymbol{u})$; $\tilde{\boldsymbol{E}}(\boldsymbol{y}_1, \boldsymbol{u})$. Hence, we have

$$\begin{aligned}\tilde{e}_2 &= \left(\tilde{\boldsymbol{A}}_{22} - \boldsymbol{H}_{22} - \tilde{\boldsymbol{E}}_2 \tilde{\boldsymbol{E}}_1^T (\boldsymbol{y}_1, \boldsymbol{u}) \left(\tilde{\boldsymbol{A}}_{12} - \boldsymbol{H}_{12}\right)\right) \tilde{e}_2 \\ &\quad + \boldsymbol{\Gamma}_2 (\tilde{\boldsymbol{x}}, \boldsymbol{u}) - \boldsymbol{\Gamma}_2 (\boldsymbol{x}, \boldsymbol{u}) - \tilde{\boldsymbol{E}}_2 \tilde{\boldsymbol{E}}_1^T (\boldsymbol{y}_1, \boldsymbol{u}) [\boldsymbol{\Gamma}_1 (\tilde{\boldsymbol{x}}, \boldsymbol{u}) - \boldsymbol{\Gamma}_1 (\boldsymbol{x}, \boldsymbol{u})]\, .\end{aligned}$$

The gain design now depends on the matrix $\boldsymbol{\Psi} = \tilde{\boldsymbol{A}}_{22} - \boldsymbol{H}_{22} - \tilde{\boldsymbol{E}}_2 \tilde{\boldsymbol{E}}_1^{\mathrm{T}} (\boldsymbol{y}_1, \boldsymbol{u})(\tilde{\boldsymbol{A}}_{12} - \boldsymbol{H}_{12})$. The conditions that will guarantee stability are reduced to the form

$$\begin{aligned}&\boldsymbol{\Psi}^T \boldsymbol{P}_2 + \boldsymbol{P}_2 \boldsymbol{\Psi} = -\boldsymbol{I} \\ &\boldsymbol{\lambda}_{\max(\boldsymbol{P}_2)} \leq \frac{1}{2\left[\boldsymbol{l}_{\Gamma 2} + \boldsymbol{b}_{\gamma 1} \boldsymbol{l}_{\Gamma 1}\right]^T}.\end{aligned}$$

6.0 FAULT RECOVERY FROM THE SLIDING MODE OBSERVER

The equivalent output error injection signal $\boldsymbol{v}_{\mathrm{eq}}$ in Equation (16) is needed for the existence of the sliding mode[6,14] and is rewritten as[31]:

$$\boldsymbol{v}_{eq} = \boldsymbol{C}_1 \boldsymbol{E} (\hat{\boldsymbol{x}}, \boldsymbol{u}))^{-1} \boldsymbol{C}_1 \boldsymbol{E} (\boldsymbol{x}, \boldsymbol{u})\, \boldsymbol{f} (\boldsymbol{t}) - \emptyset (\boldsymbol{e}, \hat{\boldsymbol{x}}, \boldsymbol{x}, \boldsymbol{u})\, , \quad \ldots (25)$$

where

$$\emptyset (\boldsymbol{e}, \hat{\boldsymbol{x}}, \boldsymbol{x}, \boldsymbol{u}) = \boldsymbol{C}_1 \boldsymbol{E} (\hat{\boldsymbol{x}}, \boldsymbol{u}))^{-1} [\boldsymbol{C}_1 (\boldsymbol{A} - \boldsymbol{L}\boldsymbol{C})\, \boldsymbol{e} + \boldsymbol{C}_1 \boldsymbol{g} (\hat{\boldsymbol{x}}, \boldsymbol{u}) - \boldsymbol{C}_1 \boldsymbol{g} (\boldsymbol{x}, \boldsymbol{u})\, . \quad \ldots (26)$$

https://doi.org/10.1017/aer.2016.5 Published online by Cambridge University Press

From Assumption 2 and Equation (21), we conclude that

$$\emptyset(\boldsymbol{e}, \hat{\boldsymbol{x}}, \boldsymbol{x}, \boldsymbol{u}) \leq \boldsymbol{b}_{\tilde{E}_1} \|\boldsymbol{C}_1\| \left(\|\boldsymbol{A} - \boldsymbol{LC}\| + \boldsymbol{l}_g\right) \|\boldsymbol{e}(\boldsymbol{t})\| \rightarrow 0 (\boldsymbol{t} \rightarrow \infty). \quad \ldots(27)$$

In order to appraise the fault signal $f(t)$ from the sliding mode, the equivalent output error injection signal $\boldsymbol{v}_{\mathrm{eq}}$ needs to be reconstructed. Using a low-pass filter for reconstructing this signal was proposed by Utkin et al in 1992. In this paper, the approach extended by Edwards(14) and yan(32) will be used to appraise $\boldsymbol{v}_{\mathrm{eq}}$. From Assumption 2, the equivalent output error injection signal $\boldsymbol{v}_{\mathrm{eq}}$ in Equation (25) can be approximated by

$$\boldsymbol{v}_{eq} \cong \boldsymbol{\rho}(0) \frac{\boldsymbol{e}_y}{\boldsymbol{e}_y + \boldsymbol{\sigma}_1 exp\{-\boldsymbol{\sigma}_2 \boldsymbol{t}\}}, \quad \ldots(28)$$

where σ_1 and σ_2 are positive constants.

By defining

$$\hat{\boldsymbol{f}}(\boldsymbol{t}) = \boldsymbol{\rho}(0) \frac{\boldsymbol{e}_y}{\left\|\boldsymbol{e}_y\right\| + \boldsymbol{\sigma}_1 exp\{-\boldsymbol{\sigma}_2 \boldsymbol{t}\}}, \quad \ldots(29)$$

and by inserting the approximation of $\boldsymbol{v}_{\mathrm{eq}}$ from Equation (28) into Equation (16), we have

$$\left\|\hat{\boldsymbol{f}}(\boldsymbol{t}) - \boldsymbol{f}(\boldsymbol{t})\right\| \leq \|\emptyset(\boldsymbol{e}, \hat{\boldsymbol{x}}, \boldsymbol{x}, \boldsymbol{u})\|. \quad \ldots(30)$$

Also, $\lim_{t \rightarrow \infty} \|\hat{f}(t) - f(t)\| = 0$.

The parameters σ_1 and σ_2 in the above equation specify the degree to which an approximation to a perfect sliding mode is obtained. In the general case, σ_1 is small and σ_2 is large(14,32). Due to the numerical procedures used in the implementation of the algorithms, the error stays within a small bound $\|e_y\| \leq \varepsilon$ around the sliding surface. In the majority of practical cases, a borderline is used to cope with the inordinate chattering and this also results in an approximated sliding surface.

7.0 ADVANTAGES OF THE PROPOSED METHOD

In the design of the proposed method, considerations have been made that have a prominent role in its practical implementation:

1. The proposed fault estimation approach is easy to implement and can be applied to a reasonably wide class of non-linear systems.
2. The proposed fault estimation/reconstruction signals are based only on the available plant input/output information and can be calculated online.
3. An actuator fault reconstruction instead of just detection is presented based on the equivalent output error injection signal.
4. This proposed method is free of undesirable chattering phenomena. Moreover, it can handle both structured and unstructured uncertainties.

https://doi.org/10.1017/aer.2016.5 Published online by Cambridge University Press

5. Another benefit of the proposed fault estimation approach is its light burden of computations, which is an important figure in practical implementation and online control cases.
6. Since the integral of the system states is not used in dynamic equations of the sliding surface, the wind-up effect will not occur in the implementation of this method.
7. To design the proposed method of fault detection in Ref. 32, a transformation matrix is used to change system space. Their proposed methods for obtaining this transformation matrix were very complicated and time consuming in terms of implementation. In our paper, to overcome these difficulties, some strategies are presented that make the transfer matrix computationally efficient.

8.0 APPLICATION TO AN HIRM AIRCRAFT SYSTEM

Consider the simplified dynamics of the HIRM aircraft at the trim values Mach: 0.8, Height: 5000 ft[33-35]. By reordering the system state variables

$$\begin{aligned}\dot{\boldsymbol{x}}(\boldsymbol{t}) &= \boldsymbol{A}x(\boldsymbol{t}) + \boldsymbol{g}(\boldsymbol{x}, \boldsymbol{u}) + \boldsymbol{E}(\boldsymbol{x}, \boldsymbol{u})\boldsymbol{f}(\boldsymbol{t}) \\ \boldsymbol{y}(\boldsymbol{t}) &= \boldsymbol{C}x(\boldsymbol{t})\end{aligned}$$

$$A = \begin{bmatrix} 0 & 0 & 0 & 1 \\ -0.367 & -0.0318 & 0.0831 & -0.0008 \\ 0 & -0.0716 & -1.4850 & 0.9848 \\ 0 & -0.2797 & -5.6725 & -1.0253 \end{bmatrix}$$

$$g(x, u) = \begin{bmatrix} 0 \\ 0 \\ \frac{F_e}{M}\left(Sinx_3/1 + x_2\right) \\ 0 \end{bmatrix}$$

$$C = \begin{bmatrix} 1 & 0 & 0 & 0 \\ 0 & 0 & 0 & 1 \end{bmatrix} \text{ and } E = \begin{bmatrix} \mu_1 \\ \mu_2 \\ \mu_3 \\ \mu_4 \end{bmatrix},$$

where the parameters F_e and M are the engine thrust and the aircraft mass, respectively. This system has four states $\boldsymbol{x} = \text{col}(\boldsymbol{x}_1, \boldsymbol{x}_2, \boldsymbol{x}_3, \boldsymbol{x}_4)$: pitch angle (rad); normalised airspeed deviation $(\boldsymbol{v}\text{-}\boldsymbol{v}_0)/\boldsymbol{v}_0$ with $\boldsymbol{v}$ and $\boldsymbol{v}_0 = 267.51$ the present airspeed (m/s) and the favourable airspeed (m/s), respectively; angle-of-attack (rad); and pitch rate (rad/s). The fault distribution matrix $\boldsymbol{E}$ is dependent on the system dynamics and is known *a priori*. The representation $\mu_1, \mu_2, \ldots, \mu_4$ is adopted for the purpose of comparison with the method in[32].

It is clear that the fault signal is observable through output $\boldsymbol{y}_1$, so $\boldsymbol{C}_1 = [1\ 0\ 0\ 0]$. The other output is $\boldsymbol{y}_2 = \boldsymbol{x}_4$. The following form of observer, with one robust term, can be developed based on Equation (2).

$$\begin{aligned}\hat{\boldsymbol{x}} &= \boldsymbol{A}\hat{x} + \boldsymbol{g}(\hat{\boldsymbol{x}}, \boldsymbol{u}) + \boldsymbol{L}(\boldsymbol{y} - \boldsymbol{C}\hat{x}) + \boldsymbol{E}(\hat{\boldsymbol{x}}, \boldsymbol{u})\boldsymbol{v}(\boldsymbol{t}) \\ \boldsymbol{v}(\boldsymbol{t}) &= -(\boldsymbol{C}_1\boldsymbol{E}(\hat{\boldsymbol{x}}, \boldsymbol{u}))^{-1}\rho(0)\,sign(\boldsymbol{C}_1\hat{\boldsymbol{x}} - \boldsymbol{C}_1\boldsymbol{x}),\end{aligned}$$

https://doi.org/10.1017/aer.2016.5 Published online by Cambridge University Press

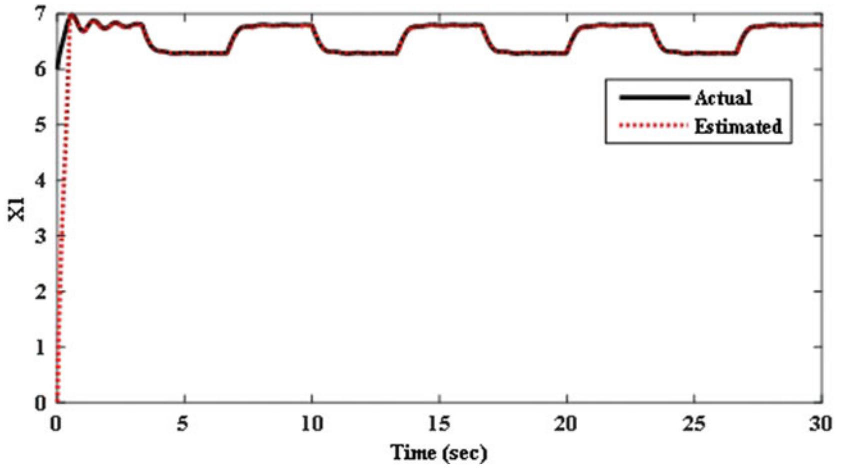

Figure 1. (Colour online) The first state of the system and the observer with a sliding-mode term.

where $\boldsymbol{L} = [\begin{smallmatrix} l_{11} & l_{21} & l_{31} & l_{41} \\ l_{12} & l_{22} & l_{23} & l_{24} \end{smallmatrix}]$ is the feedback gain in the sliding mode of $e_1 = \hat{\boldsymbol{x}}_1 - \boldsymbol{x}_1 = 0$. The unknown fault can be recovered from the sliding mode based on Equation (29) as

$$\hat{f}(\boldsymbol{t}) \cong -\frac{1}{\mu_1}\rho(0)\frac{e_1}{|e_1| + \delta}. \qquad \ldots(31)$$

9.0 SIMULATION RESULTS

To demonstrate the performance of the proposed method, simulations are presented in two stages.

Simulation 1: In this section, we try to design our proposed SMO for estimating the system's states. The fault distribution vector elements are selected to be $\mu_1 = 1.2$, $\mu_2 = 0.6$, $\mu_3 = 0.2$, $\mu_4 = 0.7$. The sliding-mode gain is selected to be $\rho(.) = 8$. The initial conditions for the plant and estimator are set as $\boldsymbol{x}(0) = [6\ 3\ 6\ 2]$ and $\hat{\boldsymbol{x}}_1(0) = [0\ 0\ 0\ 0]$, respectively. For the recovery of the unknown input from the sliding mode, the parameter δ in Equation (31) is selected to be 0.015. The gain is developed in a way that the reduced-order system is stable. We chose the feedback gain

$$\boldsymbol{L} = \begin{bmatrix} 1.701 & 0.78 & 1.6 & 0.19 \\ 0.09 & -4.65 & -4.85 & 6 \end{bmatrix}^T.$$

The positive-definite matrix $\boldsymbol{P}$ that fulfils the algebraic Ricatti equation (ARE) (28) is obtained to be

$$\boldsymbol{P} = \begin{bmatrix} 0.2494 & 0.3476 & 0.1970 \\ 0.4016 & 1.9341 & 0.8199 \\ 0.2397 & 0.2497 & 2.0091 \end{bmatrix},$$

https://doi.org/10.1017/aer.2016.5 Published online by Cambridge University Press

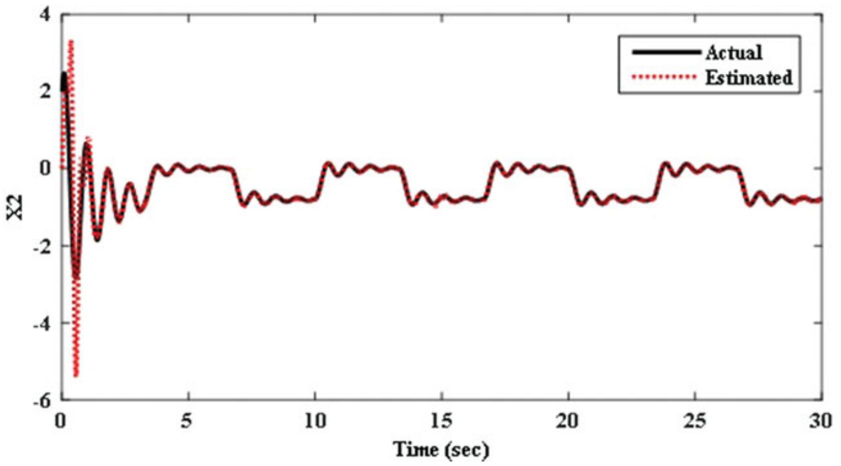

Figure 2. (Colour online) The second state of the system and the observer with a sliding-mode term.

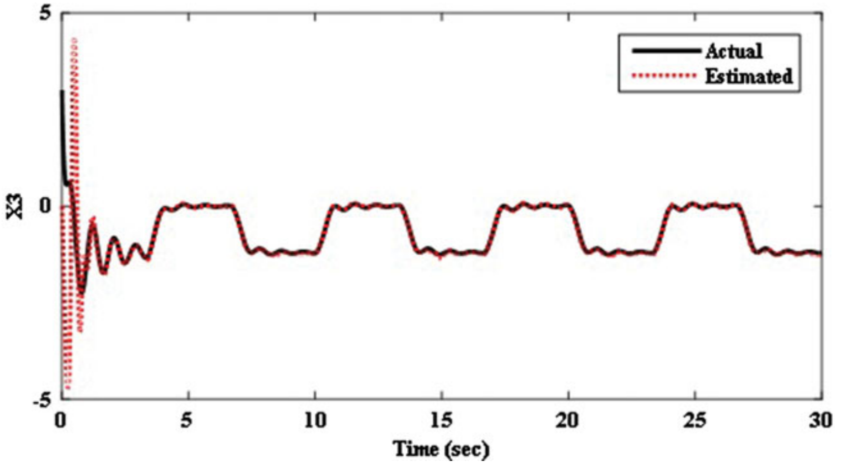

Figure 3. (Colour online) The third state of the system and the observer with a sliding-mode term.

with $\lambda_{max}(\boldsymbol{Q}) = 1.9921$. The Lipschitz constant for the selected values was computed to be $l_{\Phi} = 0.201$. Now, we can investigate if the condition in Remark 3 is fulfilled.

To verify the estimation integrity in the existence of high frequency elements, we recommend a square wave disturbance of amplitude 1 and period 6.66 s. Simulation results for the state estimation with the non-linear SMO are shown in Figs 1-4. In spite of the existence of a large unknown input/disturbance, leading to large oscillations in the HIRM aircraft, the observer was capable of tracking the states.

Simulation 2: In this stage, a fault estimator based on the proposed SMO of Yan et al (2007) is designed for an HIRM aircraft system. Then, the performance of the proposed method is compared with that of the SMO presented by Yan et al (2007) to show the superiority of the proposed method. It should be noted that the design parameters of the proposed method are the same as those in the first stage of simulation. It can be concluded from Fig. 5 that the

https://doi.org/10.1017/aer.2016.5 Published online by Cambridge University Press

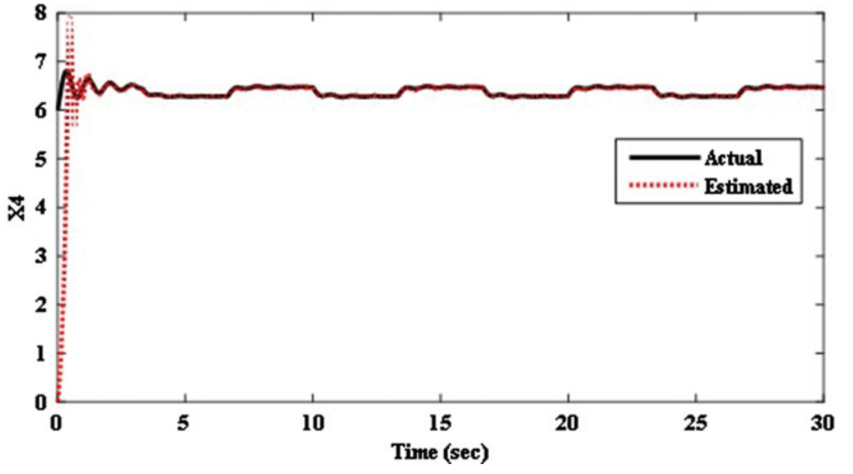

Figure 4. (Colour online) The fourth state of the system and the observer with a sliding-mode term.

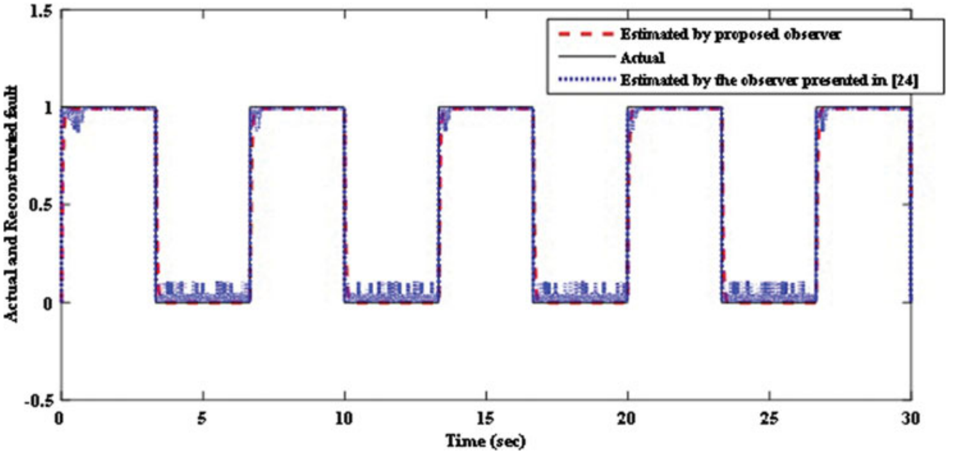

Figure 5. (Colour online) A fault and its estimation (first example).

proposed observer has estimated the fault efficiently. However, the SMO of Yan et al (2007) shows chattering and is not highly accurate. By changing the fault, as shown in Fig. 6 to verify the robustness of the suggested procedure, we selected $6\sin(0.6\pi t)–3\cos(0.35\pi t)$ as a fault signal. It can be observed that the performance of the proposed method is still acceptable. Although the SMO of Yan et al (2007) does not have chattering, it has a high estimation error making its implementation problematic.

10.0 CONCLUSION

This study aims to propose a simple SMO developed for accurate state estimation in the presence of faults for a class of non-linear systems. The proposed method is simple and is of a relatively lower complexity compared to existing methods. Robust terms are designed in a way that faults can be reconstructed directly from the sliding surfaces. Our proposed method

https://doi.org/10.1017/aer.2016.5 Published online by Cambridge University Press

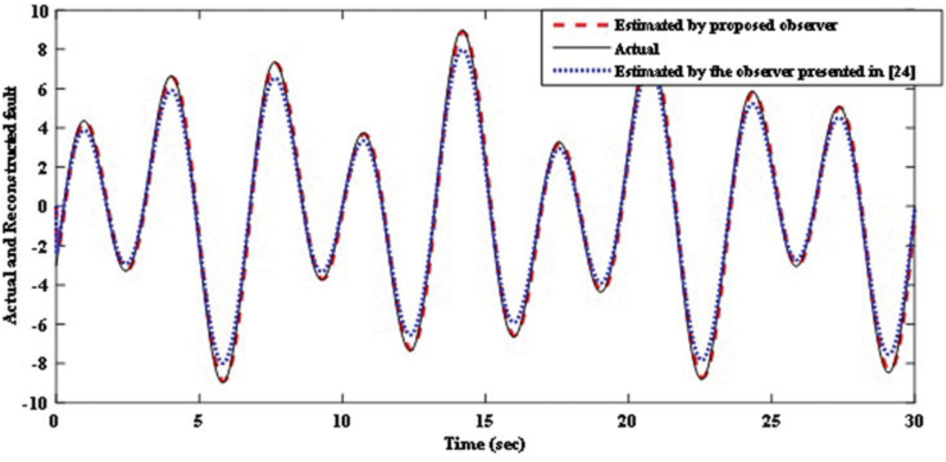

Figure 6. (Colour online) A fault and its estimation (second example).

does not need a non-linear transformation. The stability of the reduced-order error system in the sliding mode is established. A specific HIRM aircraft system example is given to illustrate the efficiency of the proposed approach. Since most industrial systems are uncertain and non-linear, extension of the proposed method to robust fault diagnosis for uncertain non-linear systems is another interesting issue.

REFERENCES

1. CHEN, J. and PATTON, R.J. *Robust Model-Based Fault Diagnosis for Dynamic Systems¸* 1999, Kluwer, Boston, Massachusetts, US.
2. KHOOBAN, M.H., SIAHI, M. and SOLTANPOUR, M.R. Model-based fault detection and estimation in robotic wheelchair using sliding mode observer, *Research J of Applied Sciences, Engineering and Technology*, 2012, **4**, (13), pp 2009-2016.
3. KALMAN, R.E. On a new approach to filtering and prediction problems. *ASME J Basic Engineering*, 1976, **24**, pp 705-718.
4. GEVERS, M. and BASTIN, G. *A Stable Adaptive Observer for a Class of Nonlinear Second-Order Systems, in Analysis and Optimization of Systems*, Bensoussan and Lions (Eds), 1986, Springer-Verlag, New York, New York, US, pp 143-155.
5. HAMMOURI, J.P. and OTHMAN, H. A simple observer for nonlinear systems, *IEEE Transactions on Automatic Control*, 1992, **37**, (6), pp 875-880.
6. UTKIN, V.I. *Sliding Modes in Control Optimization*, 1992, Springer-Verlag, Berlin, Germany.
7. WALCOTT, B.L. and ZAK, S.H. Observation of dynamical systems in the presence of bounded nonlinearities/uncertainties, Proceedings of the 25th IEEE Conference on Decision and Control, 1986, Athens, Greece, pp 961-966.
8. EDWARDS, C. and SPURGEON, S.K. On the development of discontinuous observers, *Int J of Control*, 1994, **59**, (5), pp 1211-1229.
9. THEIN, M.-W.L. and MISAWA, E.A. Comparison of the sliding observer to several state estimators using a rotational inverted pendulum, Proceedings of the 34th Conference on Decision and Control, 1995, New Orleans, Louisiana, US, pp 3385-3390.
10. FRANK, P.M. Fault diagnosis in dynamic systems using analytical and knowledge-based redundancy: A survey and some new results, *Automatica*, 1990, **26**, (3), pp 459-474.
11. MAGNI, J.F. and MOUYON, P. On residual generation by observer and parity space approaches, *IEEE Transactions on Automatic Control*, 1994, **39**, (2), p 447.
12. EDWARDS, C. and SPURGEON, S.K. *Sliding Mode Control: Theory and Applications*, 1998, CRC Press, UK.

https://doi.org/10.1017/aer.2016.5 Published online by Cambridge University Press

13. WALCOTT, B.L. and ZAK, S.H. Combined observer-controller synthesis for uncertain dynamical systems with applications, *IEEE Transactions on Systems, Man and Cybernetics*, 1988, **18**, (1), pp 88-104.
14. EDWARDS, C., SPURGEON, S.K. and PATTON, R.J. Sliding mode observers for fault detection and isolation, *Automatica*, 2000, **36**, (4), pp 541-553.
15. EDWARDS, C. and SPURGEON, S. On the development of discontinuous observers, *Int J of Control*, 1994, **59**, (5), pp 1211-1229.
16. TAN, C.P. and EDWARDS, C. An LMI approach for designing sliding mode observers, *Int J of Control*, 2001, **74**, (16), pp 1559-1568.
17. XIANG, J., SU, H. and CHU, J. On the design of Walcott-Zak sliding mode observer, Proceedings of the 2005 American Control Conference, 2005, pp 2451-2456.
18. LIN, Z., XIA, Y., SHI, P. and WU, H. Robust sliding mode control for uncertain linear discrete systems independent of time-delay, *Int J of Innovative Computing, Information and Control*, 2011, **7**, (2), pp 869-880.
19. SHI, P., XIA, Y., LIU, G.P. and REES, D. On designing of sliding-mode control for stochastic jump systems, *IEEE Transactions on Automatic Control*, 2006, **51**, (1), pp 97-103.
20. CHANG, Y.H., WU, C.I., LIN, H.W., CHEN, H.C. and CHANG, C.W. Fractional order integral sliding-mode flux observer for direct field-oriented induction machines, *Int J of Innovative Computing, Information and Control*, 2012, **8**, 7(A), pp 4851-4868.
21. KHAN, Q., BHATTI, A.I., IQBAL, M. and AHMED, Q. Dynamic integral sliding mode control for SISO uncertain nonlinear systems, *Int J of Innovative Computing, Information and Control*, 2012, **8**, 7(A), pp 4621-4633.
22. WU, L., SHIAND, P. and GAO, H. State estimation and sliding-mode control of Markovian jump singular systems, *IEEE Transactions on Automatic Control*, 2010, **55**, (5), pp 1213-1219.
23. SOLTANPOUR, M.R., ZOLFAGHARI, B., SOLTANI, M. and KHOOBAN, M.H. Fuzzy sliding mode control design for a class of nonlinear systems with structured and unstructured uncertainties, *Int J of Innovative Computing, Information and Control*, 2013, **9**, (7), pp 2713-2726.
24. MOKHTAR, S., KHOOBAN, M.H. and NIKNAM, T. A robust and simple optimal type II fuzzy sliding mode control strategy for a class of nonlinear chaotic systems. *J of Intelligent & Fuzzy Systems: Applications in Engineering and Technology*, 2014, **27**, (4), pp 1849-1859.
25. SOLTANPOUR, M.R., KHOOBAN, M.H. and SOLTANI, M. Robust fuzzy sliding mode control for tracking the robot manipulator in joint space and in presence of uncertainties, *Robotica*, 2014, **32**, (03), pp 433-446.
26. SOLTANPOUR, M.R. and KHOOBAN, M.H. A particle swarm optimization approach for fuzzy sliding mode control for tracking the robot manipulator, *Nonlinear Dynamics*, 2013, **74**, (1-2), pp 467-478.
27. SOLTANPOUR, M. R., OTADOLAJAM, P. and KHOOBAN, M. H. Robust control strategy for electrically driven robot manipulators: adaptive fuzzy sliding mode, *IET Science, Measurement & Technology*, 2014, **9**, (3), pp 322-334.
28. JIANG, B., SHI, P. and MAO, Z. Sliding mode observer-based fault estimation for nonlinear networked control systems, *Circuits, Systems, and Signal Processing*, 2011, **30**, (1), pp 1-16.
29. QIU, J., REN, M., NIU, Y., ZHAO, Y. and GUO, Y. Fault estimation for nonlinear dynamic systems, *Circuits, Systems, and Signal Processing*, 2012, **31**, (2), pp 555-564.
30. YAN, X. and EDWARDS, C. Nonlinear robust fault reconstruction and estimation using a sliding mode observer, *Automatica*, 2007, **43**, (9), pp 1605-1614.
31. VELUVOLU, K.C. and SOH, Y.C. Fault reconstruction and state estimation with sliding mode observers for Lipschitz non-linear systems, *IET Control Theory & Applications*, 2011, **5**, (11), pp 1255-1263.
32. YAN, X.G. and EDWARDS, C. Fault estimation for single output nonlinear systems using an adaptive sliding mode estimator, *IET Control Theory & Applications*, 2008, **2**, (10), pp 841-850.
33. MAGNI, J.F., BENNANI, S. and TERLOUW, J. *Robust Flight Control: A Design Challenge*, Lecture Notes in Control and Information Sciences, 224, 1997, Springer-Verlag, Berlin, Germany.
34. HUZMEZAN, M. Theory and Aerospace Applications of Constrained Model Based Predictive Control, 1998, PhD thesis, Department of Engineering, University of Cambridge, UK.
35. YAN, X. and EDWARDS, C. Robust sliding mode observer-based actuator fault detection and isolation for a class of nonlinear systems, 44th IEEE Conference on Decision and Control, and the European Control Conference 2005, 12-15 December 2005, Seville, Spain.

https://doi.org/10.1017/aer.2016.5 Published online by Cambridge University Press